Journal of Power Sources, 43–44 (1993) 569–575

Rechargeable γ-MnO_2 for lithium batteries using a sulfone-based electrolyte at 150 °C

S. Bach and N. Baffier

Laboratoire de Chimie Appliquée de l'Etat Solide, C.N.R.S. URA 302, ENSCP 11, rue Pierre et Marie Curie, 75231 Paris Cedex 05 (France)

J. P. Pereira-Ramos and R. Messina

Laboratoire d'Electrochimie, Catalyse et Synthèse Organique, C.N.R.S. UM 28, 2 rue Henri Dunant, 94320 Thiais (France)

Abstract

The electrochemical lithium intercalation in γ-MnO_2 as well as in the ramsdellite and pyrolusite phases has been studied in molten dimethylsulfone at 150 °C. Two redox steps are evidenced: in the composition range $0 < x < 0.35$–0.4, a slow decrease of the potential (3.8–3V) is observed while for 0.35–$0.4 < x < 0.9$ a voltage plateau appears at 2.95 V. Comparison of the chronopotentiometric curves for γ-MnO_2, ramsdellite and rutile forms prove that these two insertion processes cannot be assigned to lithium accommodation into ramsdellite and pyrolusite units. At this temperature, the lithium insertion process into γ-MnO_2 is found to be highly reversible on the whole lithium concentration range ($0 < x < 0.95$) and characterized by a high kinetics of lithium transport. D_{Li} evaluated from potentiometric and voltammetric measurements is in the range 5×10^{-9} cm^2 s^{-1}. During extended galvanostatic experiments performed at a discharge/charge rate of C, a high efficiency is recovered since, from an initial capacity of 300 A h kg^{-1}, about 180 A h kg^{-1} are still available after the 20th cycle.

Introduction

Manganese dioxide was originally developed as a positive electrode for commercial primary lithium cells. However, because only a low fraction of its first discharge capacity was recoverable during the following cycles, this compound was, at first, not considered as a promising cathodic material for secondary batteries [1, 2]. Since then, a great interest has been devoted to the study of Li insertion into other forms of MnO_2, and significant advances have been obtained especially in the case of composite dimensional manganese oxide (CDMO) [3, 4] and $LiMn_2O_4$ spinel-type phases [5–8].

Apart from the recent works of Ohzuku *et al.* [9–11] which have brought some new data on the electrochemical behaviour of electrochemical manganese dioxides (EMD) MnO_2 and which have given some evidence that a reversible cycling could be reached at low rates with heat-treated EMD, little is known about the reversibility of the Li insertion process in γ-MnO_2.

In the present work, we investigate the electrochemical Li intercalation into γ-MnO_2 prepared by various ways in molten dimethylsulfone at 150 °C. The enhancement of chemical and electrochemical kinetics in such a medium provides further information on the electrochemistry of γ-MnO_2 in relation to its cycling properties.

0378-7753/93/$6.00

Experimental

Sol-gel γ-MnO_2 is obtained from the ternary oxide $AMnO_2$ (A = Li) synthesized via a sol-gel process [12]. Manganese oxide gels are formed from the reduction of aqueous permanganate solutions $LiMnO_4$ (Mn(VII)) by fumaric acid $C_4O_4H_4$. Drying and calcination of the gels in which the mean oxidation state of manganese is 4, lead to the formation of the trivalent manganese $LiMnO_2$ crystalline phase. The compound $LiMnO_2$ is then transformed into γ-MnO_2 by a sulfuric acid treatment of the ternary oxide at 90 °C for 4 to 5 days [13]. Other γ-MnO_2 compounds, β-MnO_2 and ramsdellite were synthesized in the classical way [14].

Before electrochemical measurements, all the manganese oxides were heat-treated in air at 350 °C in order to remove almost all the water molecules.

The mean oxidation state 'Z' of manganese was determined by chemical titration using ferrous sulfate [15] with an accuracy of ± 0.02. The analytical values of x in MnO_x in these samples were 1.92 for γ-MnO_2 sol-gel, 1.97 for γ-MnO_2 CMD, 1.96 for γ-MnO_2 EMD, 1.99 for β-MnO_2, and 1.97 for ramsdellite.

Dimethylsulfone ($DMSO_2$) was first recrystallized in water and then twice from absolute methanol, air dried at 90 °C for 48 h and sublimated under reduced pressure (2 mm Hg) at 100 °C [16]. It was then conserved in an argon glove box. Under these conditions, the water concentration did not exceed 5×10^{-3} mol kg^{-1}. The working electrode consisted of either a stainless-steel or a gold grid with a geometric area of ≈ 0.5 cm^2 on which the samples, mixed with graphite (20 wt.%), was pressed.

Kinetics of lithium transport in γ-MnO_2

From the variation of the current peak, i_p with the sweep rate, in voltammetry studies of a reversible redox system, an average value for the chemical diffusion coefficient of Li^+ ions, D_{Li}, can be calculated using the following relation: $i_p = 0.4463FA(\Delta C)(F/RT)^{1/2}\nu^{1/2}(D_{Li})^{-1/2}$, where F, A, ΔC, and ν are respectively the Faraday constant, the geometric area (cm^2), the variation of Li content (mol cm^{-3}) and the scan rate (V s^{-1}).

D_{Li} was also measured using the current pulse relaxation technique described by Basu *et al.* [17]. The current pulses were in the range 0.1–0.5 mA and the pulse durations were between 5 and 15 s. A molar volume $V_m = 25.48$ cm^3 mol^{-1} was used.

Results and discussion

Figure 1 shows the discharge/charge behaviour of three heat-treated γ-MnO_2 (350 °C) samples. Electrochemical Li insertion into these samples results in two main steps in the potential window 3.8–2.6 V whereas only one step is usually reported for this compound at 20 °C. In the first step the potential decreases from its initial value of 3.8–3.6 V up to 3 V and about 0.35–0.4 Li^+ ions are accommodated per mole of oxide. The second step is characterized by a voltage plateau located at 2.95 V and involves the insertion of ≈ 0.5 additional Li^+ ions. Moreover, during the charge process, the same steps are recovered and a complete removal of Li^+ ions from these three γ-MnO_2 is achieved, showing for the first time a high reversibility of the whole insertion process.

Figure 2 presents the weak influence of the current density on the chronopotentiometric curves for the reduction of the sol-gel heat-treated γ-MnO_2 (350 °C). Indeed, whatever the current density, the total faradaic yield obtained is close to

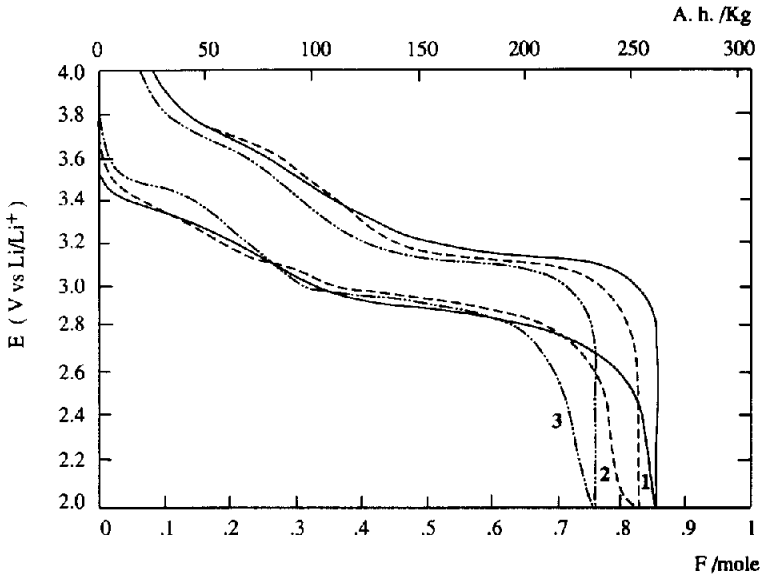

Fig. 1. Typical discharge/charge curves of (1) sol-gel γ-MnO_2, (2) EMD γ-MnO_2, and (3) CMD γ-MnO_2 (i=1 mA cm^{-2}, 1 M $LiClO_4$/$DMSO_2$ at 150 °C).

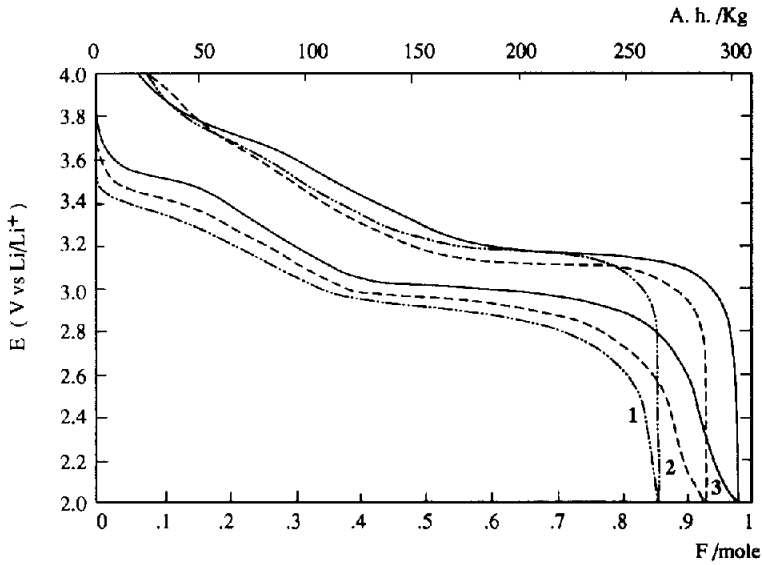

Fig. 2. Influence of the current density on the chronopotentiometric curves for the reduction of sol-gel γ-MnO_2 in 1 M $LiClO_4$/$DMSO_2$ at 150 °C: (1) i=1 mA cm^{-2}; (2) i=0.5 mA cm^{-2} and (3) i=0.1 mA cm^{-2}).

270 A h kg^{-1} ($\approx$0.9 F/Mn) which indicates a high diffusion rate of Li^+ ions in the host lattice. Owing to the mean oxidation state measured for Mn in this compound a complete reduction of all the available Mn^{4+} is evidenced by the chronopotentiometric

curve performed at a constant current density of 0.1 mA cm^{-2}; at this temperature this chronopotentiometric curve is close to the open-circuit voltage curve.

To get further information on the two steps characterizing the redox insertion process of Li into γ-MnO_2, the chronopotentiometric behaviour of β-MnO_2 and ramsdellite (Fig. 3) has been examined. β-MnO_2 has the rutile (TiO_2) structure, in which every metal atom is surrounded by six oxygen atoms. The (MnO_6) octahedra share edges to form single chains of octahedra extending along the c axis, giving a (1×1)-tunnel structure. Ramsdellite on the contrary, is built up of alternating double chains of linked (MnO_6) octahedra, giving a (2×1)-tunnel structure [18]. Comparison of the reduction curves shows that Li insertion in β-MnO_2 and ramsdellite proceeds in a quasi-similar one-step process. Indeed, a single-voltage plateau involving the reduction of all the Mn^{4+} is evidenced and is located at an energy level similar to that of the second step (2.95 V) found in the case of Li insertion in γ-MnO_2 ($0.4 < x < 0.9$). This suggests that Li^+ ions in the manganese oxide γ-MnO_2, would not be accommodated firstly into octahedral sites of the ramsdellite-type structure and then at a lower voltage into octahedral sites of the β-MnO_2-type structure. A possible correlation of the faradaic yields, obtained for the first and second steps with the ratio of ramsdellite and rutile units in any γ-MnO_2, cannot then be established. Moreover, whatever the way of synthesis in obtaining γ-MnO_2, a similar behaviour is obtained (Fig. 1). The results rather confirm the thermodynamic investigations reported by Nardi [2] and the X-ray diffraction measurements performed by Ohzuku *et al.* [9–11]. In particular, these latter structural studies indicate that the insertion reaction consists of a first step ($0 < x < 0.3$–0.5) where Li^+ ions are accommodated into a γ-MnO_2 phase having a tetragonal sublattice ($a = 4.39$–4.40 Å, $c = 2.86$–2.90 Å). This structure is then progressively converted ($0.3 < x < 0.5$) into a new Li_xMnO_2 phase having an expanding tetragonal sublattice ($a = 4.9$–5.0 Å, $c = 2.82$–2.86 Å). Further insertion occurs in this latter phase.

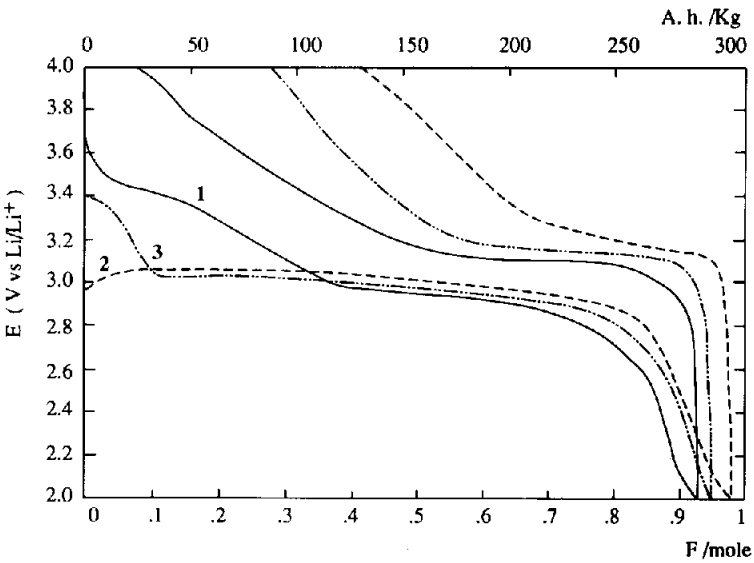

Fig. 3. Comparison of the discharge/charge curves obtained for the (1) sol-gel γ-MnO_2, (2) β-MnO_2 and (3) the ramsdellite MnO_2 ($i = 0.5$ mA cm^{-2}, 1 M $LiClO_4$/$DMSO_2$ at 150 °C).

A typical cyclic voltammogram of a γ-MnO_2 electrode is presented in Fig. 4. Electrochemical Li insertion into this compound involves two main steps at about 3.2 and 2.8 V as already shown in the chronopotentiometric study. Experimental data found for E_{pCAT}, E_{pAN}, I_{pCAT} and I_{pAN} of the second step, are summarized in Table 1. In all cases, and whatever the scanning rate, the amount of charge that is passed for the reduction and oxidation processes are practically similar; it corresponds to the quantitative reduction of the Mn^{4+} ions to Mn^{3+}. Within experimental error, no important shift of the peak potentials is found for sweep rates in the range 42×10^{-5}–1.7×10^{-5} V s^{-1}. Two identical linear relations are obtained since constant values for $I_{pCAT}/V^{1/2}$ and $I_{pAN}/V^{1/2}$ ratios are found (Table 1). This result is consistent with the existence of a reversible redox system; an average value for the chemical diffusion coefficient of Li^+ ions, $D_{Li}=6\times10^{-9}$ cm^2 s^{-1} can be determinated from the slopes of the straight lines. Experimental data found from the current pulse relaxation technique of Basu *et al.* [17] for D_{Li} give close values, $D_{Li}=4.8\times10^{-9}$ cm^2 s^{-1} for $x=0.50$ and $D_{Li}=6.5\times10^{-9}$ cm^2 s^{-1} for $x=0.65$.

Figure 5 presents the evolution of the specific capacity during extended galvanostatic cycling experiments performed at 0.5 mA cm^{-2} in the potential window 4–2 V.

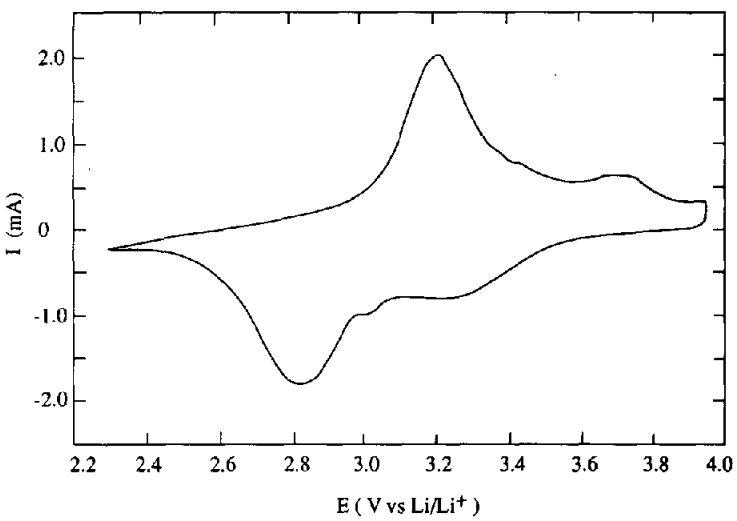

Fig. 4. Sol-gel γ-MnO_2 cyclic voltammetric curve performed between cycling limits of 3.9 and 2.3 V in 1 M $LiClO_4/DMSO_2$ at 150 °C (scanning rate was 23×10^{-5} V s^{-1}).

TABLE 1

Influence of the scanning rate on the peak potentials (E_p) and the current peaks (I_p) for the second step ($0.35–0.4 < x < 0.9$)

Scanning rate (10^5 V s^{-1})	42	33	23	8	1.7
E_{pCAT} (V) ±0.01	2.82	2.82	2.85	2.84	2.88
E_{pAN} (V) ±0.01	3.22	3.19	3.19	3.21	3.18
$I_{pCAT}/V^{1/2}$ (mA $V^{-1/2}$ $s^{1/2}$)	0.0809	0.0816	0.0799	0.0765	0.0789
$I_{pAN}/V^{1/2}$ (mA $V^{-1/2}$ $s^{1/2}$)	0.0809	0.0779	0.0808	0.0809	0.0888

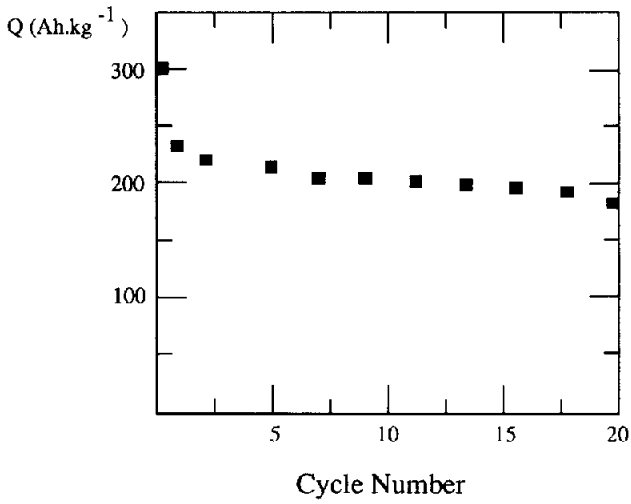

Fig. 5. Evolution of the specific capacity Q as a function of the number of cycles of sol-gel γ-MnO_2 ($i = 0.5$ mA/cm^2, discharge/charge rate: C, cycling limits: 4.0–2 V).

Interesting performances are obtained since the capacity falls to 70% of its initial value (300 A h kg^{-1}) by about the 4th cycle (210 A h kg^{-1}) to reach more slowly 180 A h kg^{-1} i.e., 60% of the initial value after the 20th cycle.

The whole results prove that the way of synthesis, γ-MnO_2 is an intrinsically reversible material for which important kinetic limitations prevail at room temperature. Two redox steps for the Li intercalation in γ-MnO_2 are evidenced for $0 < x < 0.35$–0.4 and 0.35–$0.4 < x < 0.9$. We have shown that these processes do not correspond to Li insertion into ramsdellite and pyrolusite units.

References

1 L. Li and G. Pistoia, *Solid State Ionics, 47* (1991) 231.
2 J. C. Nardi, *J. Electrochem. Soc., 132* (1985) 1787.
3 T. Nohma, T. Saito, N. Furukawa and H. Ikeda, *J. Power sources, 26* (1989) 389.
4 T. Nohma, Y. Yamamoto, K. Nishio, I. Nakane and N. Furukawa, *J. Power Sources, 32* (1990) 373.
5 J. M. Tarascon, E. Wang, F. K. Shokoohi, W. R. McKinnon and S. Colson, *J. Electrochem. Soc., 138* (1991) 2859.
6 J. M. Tarascon and D. Guyomard, *J. Electrochem. Soc., 138* (1991) 2864.
7 F. K. Shokoohi, J. M. Tarascon and B. J. Wilkens, *Appl. Phys. Lett., 59* (1991) 1260.
8 Sony's Lithium Manganese Rechargeable Battery (AA size), *JEC Battery Newsletter, 1* (1988) 26.
9 T. Ohzuku, M. Kitagawa and T. Hirai, *J. Electrochem. Soc., 137* (1989) 3169.
10 T. Ohzuku, M. Kitagawa and T. Hirai, *J. Electrochem. Soc., 137* (1990) 40.
11 T. Ohzuku, J. Kato, K. Sawai and T. Hirai, *J. Electrochem. Soc., 138* (1991) 2556.
12 S. Bach, M. Henry, N. Baffier and J. Livage, *J. Solid State Chem., 88* (1990) 325.
13 M. M. Thackeray and A. de Kock, *J. Solid State Chem., 74* (1988) 414.
14 K. M. Parida, S. B. Kanungo and B. R. Sant, *Electrochim. Acta, 26* (1981) 435.
15 M. J. Katz, R. C. Clarke and W. F. Nye, *Anal. Chem., 28* (1956) 507.

16 J. P. Pereira-Ramos, *Thesis*, Paris, 1988.
17 S. Basu and W. L. Worrel, in P. Vashita, J. N. Mundy and G. K. Shenoy (eds.), *Fast Ion Transport in Solids*, Elsevier, Amsterdam, 1979, p. 149.
18 R. G. Burns and V. M. Burns, *Manganese Dioxide Symposium, Cleveland, OH, USA*, 1975, p. 306.